Articles

Electrostatically Assembled Fluorescent Thin Films of Rare-Earth-Doped Lanthanum Phosphate Nanoparticles

Peter Schuetz and Frank Caruso*

Max Planck Institute of Colloids and Interfaces, D-14424 Potsdam, Germany

Received June 3, 2002. Revised Manuscript Received August 2, 2002

We report on the formation of nanostructured, ultrathin films of a new class of fluorescent nanoparticles (NPs) within the same size range as quantum dots, but with a different kind of fluorescence, by using the layer-by-layer (LbL) technique. The fluorescence of these rare-earth-doped lanthanum phosphate ($LaPO_4$) NPs is due to the bulk properties of the material and is therefore independent of their size. Additionally, different colors are available due to variation of the dopants used in their synthesis (e.g., Ce, Tb, Eu, and Dy). These NPs were electrostatically assembled to form thin films on planar quartz supports as well as on polystyrene (PS) microspheres with the aid of oppositely charged polyelectrolyte interlayers. Regular growth of the multilayers was observed on both quartz and PS substrates, providing control over the composition and, in turn, the fluorescence intensity of the planar films and composite spheres. The resulting films exhibit the same UV and fluorescence characteristics as the corresponding aqueous NP dispersions. NPs with different fluorescence characteristics (i.e., colors) retain their individual optical properties when premixed and assembled into thin films and can be detected individually using only a single excitation wavelength. Biofunctionalization of $LaPO_4$ NP-tagged PS spheres and of the individual $LaPO_4$ NPs is expected to yield versatile labels that could be exploited in various biological applications.

Introduction

Metal and semiconductor nanoparticles (NPs) play a major role in the development of functional nanoscale materials and devices.[1−4] They have been widely exploited as building blocks to realize a range of NP architectures, including two- and three-dimensional film assemblies,[5−13] designed colloidal aggregates,[14−17] and NP-based photovoltaic,[18,19] electroluminescence,[20−22] and sensing[23] devices. A major attribute of such NPs is their size-dependent physicochemical (e.g., optical, electrical, magnetic, and catalytic) properties. For example, semiconductor nanoparticles (or QDs) such as CdTe or CdSe, typically in the range of 1.5−4 nm,[24−27] show unique absorption and fluorescence characteristics due to quantum size effects.[28,29] QDs can be excited efficiently at a single wavelength, emitting at distinctly different wavelengths from the visible to the near-IR with small

* To whom correspondence should be addressed. Tel.: +49 331 567 9410. Fax: +49 331 567 9202. E-mail: frank.caruso@mpikg-golm.mpg.de.

(1) Niemeyer, C. M. Angew. Chem., *Int. Ed*. **2001**, *40*, 4128.
(2) Shipway, A. N.; Katz, E.; Willner, I. *ChemPhysChem* **2000**, *1*, 18.
(3) Schmid, G., Ed. *Clusters and Colloids. From Theory to Applications*; Wiley-VCH: Weinheim, 1994.
(4) Fendler, J. H., Ed. *Nanoparticles and Nanostructured Films. Preparation, Characterization and Applications*; Wiley-VCH: Weinheim, 1998.
(5) Kiely, C. J.; Fink, J.; Brust, M.; Bethell, D.; Schiffrin, D. J. *Nature* **1998**, *396*, 444.
(6) Whetten, R. L.; Khoury, J. T.; Alvarez, M. M.; Murthy, S.; Vezmar, I.; Wang, Z. L.; Stephens, P. W.; Cleveland, C. L.; Luedtke, W. D.; Landman, U. *Adv. Mater.* **1996**, *8*, 428.
(7) Giersig, M.; Ung, T.; LizMarzan, L. M.; Mulvaney, P. *Adv. Mater.* **1997**, *9*, 570.
(8) Gittins, D. I.; Bethell, D.; Nichols, R. J.; Schiffrin, D. J. *Adv. Mater*. **1999**, *11*, 737.
(9) Schmitt, J.; Decher, G.; Dressick, W. J.; Brandow, S. L.; Geer, R. E.; Shashidhar, R.; Calvert, J. M. *Adv. Mater*. **1997**, *9*, 61.
(10) Feldheim, D. L.; Grabar, K. C.; Natan, M. J.; Mallouk, T. E. *J. Am. Chem. Soc.* **1996**, *118*, 7640.
(11) Cassagneau, T.; Fendler, J. H. *J. Phys. Chem. B* **1999**, *103*, 1789.
(12) Velev, O. D.; Tessier, P. M.; Lenhoff, A. M.; Kaler, E. W. *Nature* **1999**, *401*, 548.
(13) Jiang, P.; Cizeron, J.; Bertone, J. F.; Colvin, V. L. *J. Am. Chem. Soc.* **1999**, *121*, 7957.
(14) Alivisatos, A. P.; Johnsson, K. P.; Peng, X. G.; Wilson, T. E.; Loweth, C. J.; Bruchez, M. P.; Schultz, P. G. *Nature* **1996**, *382*, 609.
(15) Mirkin, C. A.; Letsinger, R. L.; Mucic, R. C.; Storhoff, J. J. *Nature* **1996**, *382*, 607.
(16) Shenton, W.; Davis, S. A.; Mann, S. *Adv. Mater.* **1999**, *11*, 449.
(17) Connolly, S.; Fitzmaurice, D. *Adv. Mater.* **1999**, *11*, 1202.
(18) Wang, Y.; Herron, N. *Chem. Phys. Lett.* **1992**, *200*, 71.
(19) Kotov, N. A.; Dekany, I.; Fendler, J. H. *J. Phys. Chem*. **1995**, *99*, 13065.
(20) Mattoussi, H.; Radzilowski, L.; Dabbousi, B. O.; Thomas, E. L.; Bawendi, M. G.; Rubner, M. F. *J. Appl. Phys.* **1998**, *83*, 7965.
(21) Colvin, V.; Schlamp, M. C.; Alivisatos, A. *Nature* **1994**, *370*, 345.
(22) Gao, M.; Richter, B.; Kirstein, S. *Adv. Mater.* **1997**, *9*, 802.
(23) Park, S. J.; Taton, T. A.; Mirkin, C. A. *Science* **2002**, *295*, 1503.
(24) Chan, W. C. W.; Nie, S. M. *Science* **1998**, *281*, 2016.
(25) Bruchez, M.; Moronne, M.; Gin, P.; Weiss, S.; Alivisatos, A. P. *Science* **1998**, *281*, 2013.
(26) Weller, H. *Adv. Mater*. **1993**, *5*, 88.
(27) Alivisatos, A. P. *Science* **1996**, *271*, 933.
(28) Brus, L. *J. Chem. Phys*. **1984**, *80*, 4403.
(29) Henglein, A. *Ber. Bunsen-Ges. Phys. Chem*. **1995**, *99*, 903.

10.1021/cm0212257 CCC: $22.00
Published on Web 09/21/2002

variations in their size (on the order of several nanometers).

An alternative class of NPs that exhibit unique optical properties are those based on rare-earth-doped lanthanum phosphates ($LaPO_4$).[30,31] Recently, a synthesis route in organic solvent for highly monodisperse fluorescent $LaPO_4$ NPs was reported by Riwotzki et al.[32] These NPs were subsequently transferred to an aqueous phase by use of various stabilizing agents.[33] Despite being in the same size range (≈5 nm) as QD NPs, the fluorescence of $LaPO_4$ NPs is of a completely different nature. Whereas semiconductor NPs are fluorescent due to size-dependent band gaps, the fluorescence of the $LaPO_4$ NPs originates from their bulk properties (i.e., transitions between d and f electron states and their local symmetry).[32,34,35] In contrast to QDs, their spectral (absorbance and emission) properties can be tuned by the rare-earth dopant used, thus yielding NPs with different optical properties regardless of their size. Other features of $LaPO_4$ NPs are their high quantum yield (up to 61%),[34] their high chemical stability, and their expected low toxicity,[36] making them potentially suitable for biological labeling applications. Additionally, rare-earth-doped $LaPO_4$ thin films from micrometer-sized powders have long been applied as coatings for luminescent lamps,[35,37] emphasizing their high stability toward bleaching.

The ability to build layered structures of fluorescent NPs with nanoscale precision and adjustable properties is a key requirement for the preparation of functional thin film devices.[18−22] One of the most prominent approaches for obtaining vertically structured thin films with control at the nanometer level is the layer-by-layer (LbL) assembly technique.[38−40] The basis of the method is the sequential deposition of oppositely charged species onto a substrate. This technique, first introduced in 1991 by Decher and Hong for pure polyelectrolyte multilayers,[38] has in recent years been expanded to include a wide range of different building blocks (e.g., nanoparticles), substrates, interactions, and solvents.[41] For example, the LbL strategy has been employed to build structured multilayers of NPs of gold,[9,42] various oxides (magnetite[43] and silica[44]), semiconductors (CdS,[45] CdSe,[22] CdTe,[46,47] and HgTe[48]), as well as of fullerenes[49] and polyelectrolyte complexes.[50] The LbL assembly of NPs on colloidal spheres has also been demonstrated for various NPs, including silica,[51−53] gold,[54−56] iron oxide,[57,58] semiconductor,[59,60] and core-shell nanoparticles.[61]

In this article, we examine the LbL assembly of $LaPO_4$ NPs (doped with different rare-earth ions) in alternation with oppositely charged polyelectrolytes onto both planar and spherical (colloidal) supports. The motivation of this work was to gain an understanding of the NP adsorption properties, to investigate their incorporation into multilayer thin films, and to examine the optical properties of the prepared films. The NPs, ≈6 nm in diameter, have three distinct colors, as seen by the eye under UV illumination: green (Ce/Tb-doped), red (Eu-doped), and yellow (Ce/Dy-doped). We utilized the NPs to prepare ultrathin films with defined optical (fluorescence) properties, composition, and thickness. It is shown that the NPs retain their individual optical characteristics, even when assembled as NP comixtures. The $LaPO_4$ NPs and the NP-labeled beads are expected to be of widespread interest for various biological applications following their conjugation with proteins.

Experimental Section

Materials. Quartz substrates for UV−vis and fluorescence measurements were purchased from Hellma, Jena, Germany. 9-MHz gold-coated quartz crystal microbalance (QCM) electrodes were obtained from Kyushu Dentsu, Nagasaki, Japan. The PS spheres of diameter 640 nm were synthesized in house according to the method of Furusawa et al.[62] The polyelectrolytes, sodium poly(styrene sulfonate) (PSS) (M_W 70 000), poly(dimethyldiallylammonium chloride) (PDDA) (M_W 100 000), and poly(ethylenimine) (PEI) (M_W 25 000) were obtained from Sigma-Aldrich. PSS was dialyzed against Milli-Q water (M_W cutoff 14 000) and lyophilized prior to use. The $LaPO_4$ NPs (REN-X) were kindly supplied by Nanosolutions GmbH, Hamburg, Germany. Aqueous stock solutions with a concentration of ≈1 wt % were used. The water for all experiments

(30) Lenggoro, I. W.; Xia, B.; Mizushima, H.; Okuyama, K.; Kijima, N. *Mater. Lett.* **2001**, *50*, 92.
(31) Meyssamy, H.; Riwotzki, K.; Kornowski, A.; Naused, S.; Haase, M. *Adv. Mater.* **1999**, *11*, 840.
(32) Riwotzki, K.; Meyssamy, H.; Kornowski, A.; Haase, M. *J. Phys. Chem. B* **2000**, *104*, 2824.
(33) Haubold, S.; Haase, M.; Riwotzki, K.; Weller, H.; Meyssamy, H.; Ibarra, F. WO 0220696, 2002.
(34) Riwotzki, K.; Meyssamy, H.; Schnablegger, H.; Kornowski, A.; Haase, M. *Angew. Chem., Int. Ed.* **2001**, *40*, 573.
(35) Bourcet, J. C.; Fong, F. K. *J. Chem. Phys.* **1974**, *60*, 34.
(36) Hutchison, A. J. *Peritoneal Dial. Int.* **1999**, *19*, S408. On the basis of this and other studies using lanthanum ions for medical applications, $LaPO_4$ NPs are expected to show low toxicity.
(37) Hashimoto, N.; Takada, Y.; Sato, K.; Ibuki, S. *J. Lumin.* **1991**, *48−49*, 893.
(38) Decher, G.; Hong, J. D. *Ber. Bunsen-Ges. Phys. Chem.* **1991**, *95*, 1430.
(39) Decher, G.; Hong, J. D.; Schmitt, J. *Thin Solid Films* **1992**, *210−211*, 831.
(40) Decher, G. *Science* **1997**, *277*, 1232.
(41) Bertrand, P.; Jonas, A.; Laschewski, A.; Legras, R. *Macromol. Rapid Commun.* **2000**, *21*, 319.
(42) Liu, Y.; Wang, Y.; Claus, R. O. *Chem. Phys. Lett.* **1998**, *298*, 315.
(43) Mamedov, A. A.; Kotov, N. A. *Langmuir* **2000**, *16*, 5530.
(44) Lvov, Y.; Ariga, K.; Onda, M.; Ichinose, I.; Kunitake, T. *Langmuir* **1997**, *13*, 6195.
(45) Halaoui, L. I. *Langmuir* **2001**, *17*, 7130.
(46) Lesser, C.; Gao, M.; Kirstein, S. *Mater. Sci. Eng. C* **1999**, *8−9*, 159.
(47) Mamedov, A. A.; Belov, A.; Giersig, M.; Mamedova, N. N.; Kotov, N. A. *J. Am. Chem. Soc.* **2001**, *123*, 7738.
(48) Rogach, A. L.; Koktysh, D. S.; Harrison, M.; Kotov, N. A. *Chem. Mater.* **2000**, *12*, 1526.
(49) Luo, C.; Guldi, D. M.; Maggini, M.; Menna, E.; Mondini, S.; Kotov, N. A.; Prato, M. *Angew. Chem., Int. Ed.* **2000**, *39*, 3905.
(50) Schuetz, P.; Caruso, F. *Colloids Surf. A* **2002**, *207*, 33.
(51) Caruso, F.; Caruso, R. A.; Möhwald, H. *Science* **1998**, *282*, 1111.
(52) Caruso, F.; Lichtenfeld, H.; Möhwald, H.; Giersig, M. *J. Am. Chem. Soc.* **1998**, *120*, 8523.
(53) Caruso, F.; Möhwald, H. *Langmuir* **1999**, *15*, 8276.
(54) Dokoutchaev, A.; James, J. T.; Koene, S. C.; Pathak, S.; Prakash, G. K. S.; Thompson, M. E. *Chem. Mater.* **1999**, *11*, 2389.
(55) Oldenburg, S. J.; Averitt, R. D.; Westcott, S. L.; Halas, N. *J. Chem. Phys. Lett.* **1998**, *288*, 243.
(56) Gittins, D. I.; Susha, A. S.; Schoeler, B.; Caruso, F. *Adv. Mater.* **2002**, *14*, 508.
(57) Caruso, F.; Susha, A. S.; Giersig, M.; Möhwald, H. *Adv. Mater.* **1999**, *11*, 950.
(58) Caruso, F.; Spasova, M.; Susha, A.; Giersig, M.; Caruso, R. A. *Chem. Mater.* **2001**, *13*, 109.
(59) Susha, A.; Caruso, F.; Rogach, A. L.; Sukhorukov, G. B.; Kornowski, A.; Möhwald, H.; Giersig, M.; Eychmüller, A.; Weller, H. *Colloids Surf. A* **2000**, *163*, 39.
(60) Rogach, A.; Susha, A.; Caruso, F.; Sukhorukov, G.; Kornowski, A.; Kershaw, S.; Möhwald, H.; Eychmüller, A.; Weller, H. *Adv. Mater.* **2000**, *12*, 333.
(61) Caruso, F.; Spasova, M.; Salgueirino-Maceira, V.; Liz-Marzan, L. M. *Adv. Mater.* **2001**, *13*, 1090.
(62) Furusawa, K.; Norde, W.; Lyklema, J. *Kolloid-Z. Z. Polym.* **1972**, *250*, 908.

was prepared in a Milli-Q system and had a resistivity higher than 18.2 MΩ cm.

Substrate Preparation. All substrates used were cleaned prior to use according to the following procedures. Quartz slides (for UV−vis experiments) and silicon wafers (for AFM measurements) were first cleaned by ultrasonication in 2-propanol for 5 min. They were then hydrophilized by immersion in a solution containing 100 mL of NH_4OH (29 wt % aqueous solution), 100 mL of H_2O_2 (30 wt % aqueous solution), and 500 mL of water at 70 °C for 10 min, followed by rinsing with copious amounts of water. (Caution: Mixtures of ammonium hydroxide and hydrogen peroxide are extremely corrosive.) The gold-coated QCM electrodes were prepared for adsorption experiments by etching them with piranha solution (0.1 mL of 30% H_2O_2 to 0.2 mL of concentrated sulfuric acid) for 1 min and washing them thoroughly with water.[63] (Caution: Aggressive solution; use with care and prepare only small quantities.) The connecting wires were then coated with silicone paste (to prevent rusting when exposed to salt solutions for prolonged periods of time) and allowed to dry overnight prior to use.

$LaPO_4$ NP Assembly on Planar Substrates. Multilayers were formed by the electrostatic LbL assembly of oppositely charged $LaPO_4$ NPs and polyelectrolytes as follows. All substrates were first primed with a layer of PEI by exposing them to a 1 mg mL^{-1} solution for 20 min and rinsing several times with water. Three additional layers, PSS, PDDA, and finally PSS, were then assembled by consecutively dipping the PEI-coated slides into the respective polyelectrolyte solutions (1 mg mL^{-1} containing 0.5 M NaCl) for at least 20 min, after which they were removed, rinsed thoroughly with deionized water, and dried in a nitrogen flow. The NPs were then adsorbed for 60 min from a solution prepared by diluting the stock dispersion with deionized water by a factor of 20, followed by rinsing and drying (as outlined above). The adsorption time of 60 min was found to be sufficient to give NP saturation coverage of the surface (see later). Additional PSS/$LaPO_4$ NP bilayers were deposited by using the above-mentioned procedures, thus yielding $LaPO_4$ NP-based multilayer films.

$LaPO_4$ NP Assembly on Colloids. Multilayers of polyelectrolytes and $LaPO_4$ NPs were adsorbed on 640-nm-diameter PS spheres using the LbL method. The microspheres were first precoated with four polyelectrolyte layers [$(PDDA/PSS)_2$] to provide a uniformly charged surface and one that is identical to that of the coated quartz slides. The polyelectrolytes were alternately deposited from solutions containing 0.5 M sodium chloride for 20 min, followed by four cleaning cycles of centrifugation and redispersion in water. For coating with the NPs, 0.25 mL of the dispersion of PS spheres, containing $\approx 5 \times 10^8$ spheres, was added to a diluted NP solution (0.05 mL of the stock $LaPO_4$ NP solution in 0.95 mL of water). This mixture was placed on a shaker for 1 h and then cleaned six times by centrifugation and redispersion of the pellet in water.

Transmission Electron Microscopy (TEM). Approximately 3 μL of the diluted particle suspensions were dried on carbon-coated copper grids. TEM images were then taken with a Zeiss EM 912 Omega microscope at an acceleration voltage of 120 kV.

Microelectrophoresis Measurements. The electrophoretic mobility of the NPs was measured with a Zetasizer 4 (Malvern Instruments, Malvern, Worcestershire, UK) by taking the average of five measurements at the stationary level.[64]

AFM Measurements. AFM images were recorded with a Nanoscope IIIa multimode microscope (Digital Instruments Inc., Santa Barbara, CA). Measurements were performed in air on "dry films" using tapping mode. Silicon tips (Nanosensors, Wetzlar) with a resonance frequency of ≈300 kHz and a spring constant of 32−41 N/m were used.

Quartz Crystal Microgravimetry (QCM). A QCM setup using a frequency counter (HP 53131A) and a home-built oscillator for 9-MHz QCM electrodes was used for measurements. The amount of material deposited on a QCM electrode is directly proportional to the observed QCM frequency shift and can be calculated using the Sauerbrey equation,[65] as described in previous work.[66] In our systems, a frequency decrease of 5 Hz corresponds to a mass uptake of 4.3 ng (electrode area = 0.16 cm^2).

UV−Vis and Fluorescence Measurements. UV−vis spectra of films prepared on quartz substrates were recorded on a HP 8453 spectrophotometer. Fluorescence spectra of the NP films on quartz supports, the aqueous dispersions of the NPs, and the NP-labeled PS spheres were obtained using a Spex Fluorolog-2 (model FL-2T2) spectrofluorimeter (ISA, Olching, Germany). Excitation wavelengths of either 255 or 274 nm were used. For most measurements, a WG 335 filter was used (inserted into the beam between the sample and detector).

Results and Discussion

Physicochemical Properties of $LaPO_4$ NPs. The NPs were synthesized according to the method of Riwotzki et al.[32] and then made water-soluble with the aid of diethylene glycol as the stabilizing agent. This results in hydrophilization of the NPs. Microelectrophoresis measurements of the diluted dispersions revealed a positively charged NP surface with a ζ-potential of about +15 mV. The positive surface charge most likely originates from the ammonium groups on the surface, as trioctylamine is used in their synthesis.[32] Samples with three different combinations of dopants, resulting in different colors, were used in this work: Ce/Tb-doped NPs (green), Eu-doped NPs (red), and Ce/Dy-doped NPs (weakly yellow), denoted as g-NPs, r-NPs, and y-NPs, respectively. A photograph of these dispersions is shown in Figure 1. The samples were diluted to about 0.05 wt % and illuminated using a 255-nm UV lamp. The perceived color of the dispersions (the green and especially the yellow NPs) under UV illumination is different from that viewed by the naked eye because of the spectral sensitivity of the digital camera used to record the images. Without UV illumination the NP dispersions are clear, even at concentrations as high as 1 wt %, highlighting the excellent homogeneity of the samples and the absence of large aggregates of the NPs. This was confirmed by TEM images, which show a mean NP size of ≈6 ± 1 nm (Figure 2). Both TEM and microelectrophoresis analyses indicated that both the $LaPO_4$ NP size and surface charge were the same, regardless of the different dopants used in their preparation.

Formation of $LaPO_4$ NP Films on Planar (Quartz) Substrates. To examine the adsorption behavior of the NPs, the fluorescence intensity of NP films formed on PEI/PSS/PDDA/PSS-coated quartz substrates as a function of NP adsorption time was monitored (Figure 3). The differently doped NPs (i.e., g-, r-, and y-NPs) all showed the same adsorption behavior: An asymptotic trend was observed, with the onset of saturation occurring after ≈60 min. This rather long saturation time can be ascribed to infiltration of the NPs into the underlying polyelectrolyte layers as well as any rearrangement of the layers upon NP adsorption. To investigate the contribution of NP infiltration, the NPs

(63) Caruso, F.; Serizawa, T.; Furlong, D. N.; Okahata, Y. *Langmuir* **1995**, *11*, 1546.
(64) Caruso, F.; Schüler, C. *Langmuir* **2000**, *16*, 9595.
(65) Sauerbrey, G. *Z. Phys.* **1959**, *155*, 206.
(66) Caruso, F.; Niikura, K.; Furlong, D. N.; Okahata, Y. *Langmuir* **1997**, *13*, 3422.

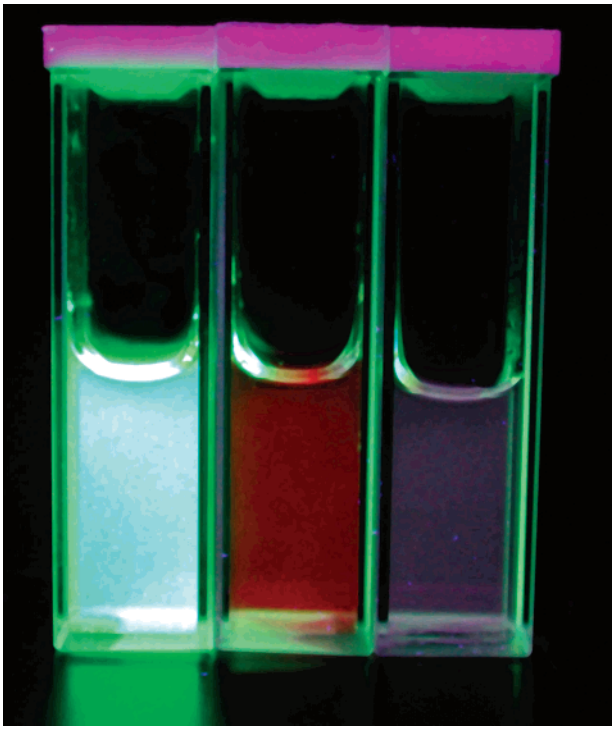

Figure 1. Photograph of fluorescent dispersions of dilute $LaPO_4$ NPs (≈0.05 wt %). From left to right: Ce/Tb-doped (green) NPs; Eu-doped (red) NPs; Ce/Dy-doped (yellow) NPs. An excitation wavelength of 255 nm was used for illumination. The color of the dispersions appear different in the photograph than they do to the naked eye under UV illumination due to the spectral sensitivity of the digital camera used to obtain the photos.

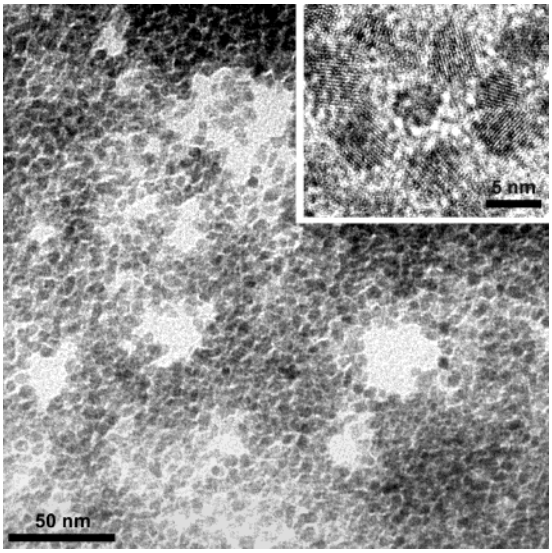

Figure 2. TEM image of $LaPO_4$ NPs (g-NPs) dried from an aqueous solution, illustrating their high monodispersity. The close packing of NPs seen is due to the high concentration of NPs dried on the TEM grid. The inset shows a higher magnification of the NPs, revealing their crystalline nature. The r- and y-NPs were identical in shape and size to those shown.

were adsorbed on preformed multilayers of different thicknesses (Figure 3 inset). The adsorbed mass for the NP adsorption step was found to be independent of the number of preassembled layers (4, 8, and 20 layers correspond to 6, 12, and 30 nm, respectively).[67] Therefore, NP adsorption only occurs at and/or in the few

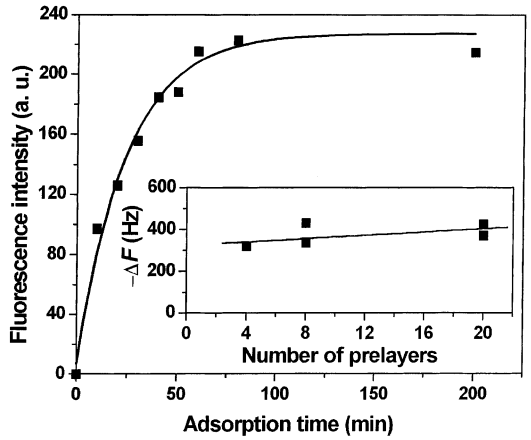

Figure 3. Adsorption isotherm for the Ce/Tb-doped (green) NPs on a quartz substrate coated with four polyelectrolyte (PEI/PSS/PDDA/PSS) layers. NP saturation is observed for adsorption times longer than 60 min. An excitation wavelength of 273 nm was used and the emission was recorded at 494 nm. The inset shows results for infiltration experiments: the (green) NPs were adsorbed on preformed PSS/PDDA films of different thicknesses on quartz. The adsorbed mass is independent of the number of preassembled layers (i.e., prelayers). The solid line is drawn as a guide to the eye.

topmost layers; that is, the NPs do not penetrate deeper into the films than maximally four layers or ≈6 nm.

The absorption properties of the aqueous NP dispersions (Figure 4a) were compared with those of the NPs adsorbed on polyelectrolyte-modified quartz substrates (Figure 4b). As the UV−vis absorption of the NP films on the substrates is quite low, these measurements were made for multilayer films comprising four layers of NPs [PEI/PSS/PDDA/(PSS/NPs)$_4$]. (Details of the formation and characterization of the multilayer films are given below.) The spectra of the green (Ce/Tb-doped) and the yellow (Ce/Dy-doped) $LaPO_4$ NPs show identical, intense peaks at 257 and 274 nm (Figure 4a), which are due to the absorption of the cerium dopant.[34] The same NPs, when assembled in a film in alternation with PSS also display these two characteristic peaks (Figure 4b). In contrast, the Eu-doped NPs in the films show no distinct absorption peaks (data not shown), as expected from the absence of a pronounced peak even in the more concentrated NP dispersions (Figure 4a).

To characterize the fluorescence of the $LaPO_4$ NP-based films, emission spectra of films containing *one layer* of NPs deposited onto PEI/PSS/PDDA/PSS-modified quartz were recorded. Figure 5 shows the emission spectra of the NPs in thin films (solid spectra) and the corresponding dispersions (dashed spectra). For the NP dispersions, in the spectral range 520−640 nm, peaks are observed at 545, 585, and 622 nm for the g-NPs (a), at 572 nm for the y-NPs (b), and at 590 and 615 nm for the r-NPs (c). Additional peaks were also observed at 490 nm (g-NPs), 479 nm (y-NPs), and ∼700 nm (r-NPs) (not shown).[68] The characteristic fluorescence peaks of the NPs in the films are also discernible, and they appear at essentially the same spectral positions as

(67) Caruso, F.; Lichtenfeld, H.; Donath, E.; Möhwald, H. *Macromolecules* **1999**, *32*, 2317.

(68) The spectral range from 480 to 520 nm is not shown, as the use of a filter was required to eliminate excitation light. With a filter in place, the intensity of the peaks for the samples shown in Figure 5 could not be clearly observed.

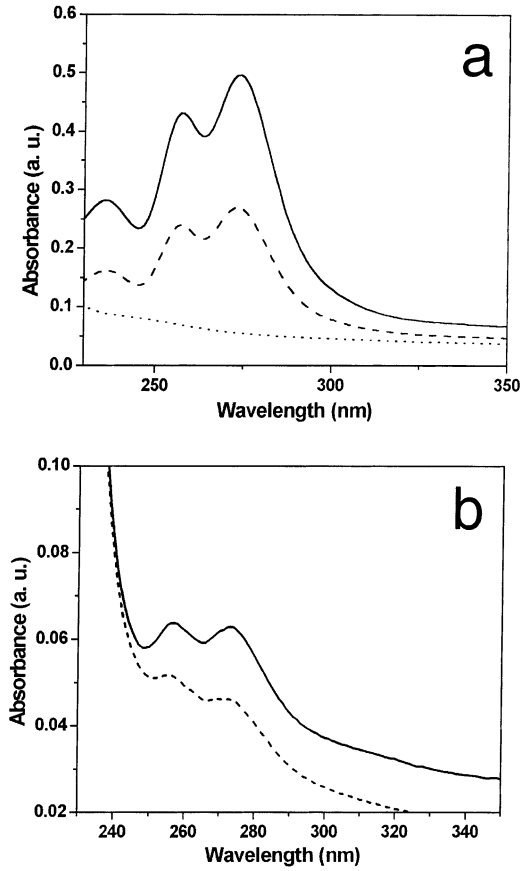

Figure 4. UV−vis spectra of the $LaPO_4$ NP dispersions in water (a) and the same NPs adsorbed on PEI/PSS/PDDA/PSS-modified quartz slides (b). As the absorption of one NP layer is relatively weak, spectra of multilayer films were recorded (film composition: PEI/PSS/PDDA/$(PSS/NPs)_4$) (b). In both parts of the figure, the solid spectra represent green NPs, while the dashed and the dotted spectra correspond to yellow and red NPs, respectively.

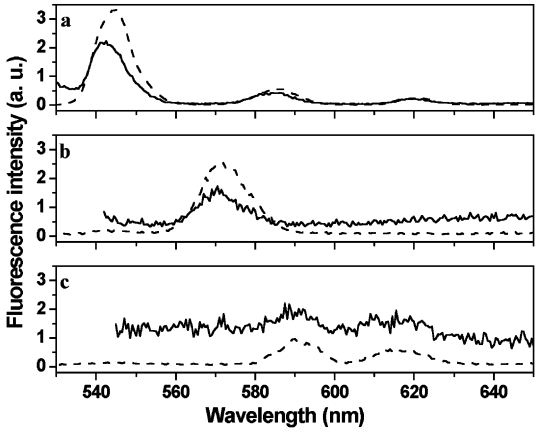

Figure 5. Fluorescence spectra for the different NPs in aqueous solution (dashed spectra) and deposited onto PEI/PSS/PDDA/PSS-modified quartz substrates (solid spectra): (a) g-NPs, (b) y-NPs, and (c) r-NPs. An excitation wavelength of 255 nm was used.

those for the corresponding NPs in solution. The fluorescence peaks are all due to the d−f transitions of the dopants.[32,34] The morphology of the NP films was also examined by AFM. The films were found to resemble those of the underlying polyelectrolyte (PEI/PSS/PDDA/PSS) film. This is probably due to a combination of the small size of the NPs, enabling their infiltration into the top few polyelectrolyte layers (see above) and the (large) size of the AFM tip.

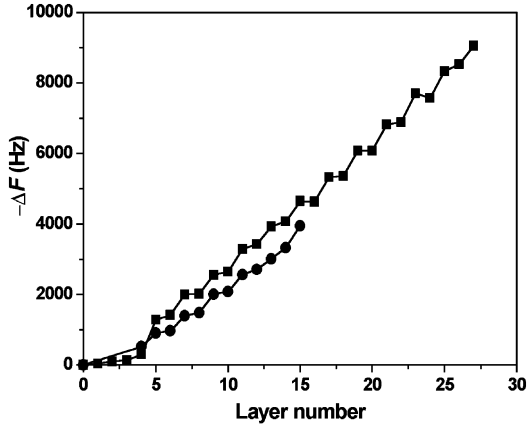

Figure 6. QCM measurements showing the growth (via frequency changes, $-\Delta F$) of layers of $LaPO_4$ NPs alternating with PSS. The squares correspond to g-NPs and the circles to r-NPs. The negative ΔF values indicate an increase in adsorbed material on the QCM surface. The odd layer numbers correspond to the NP adsorption steps and the even layer numbers to PSS adsorption.

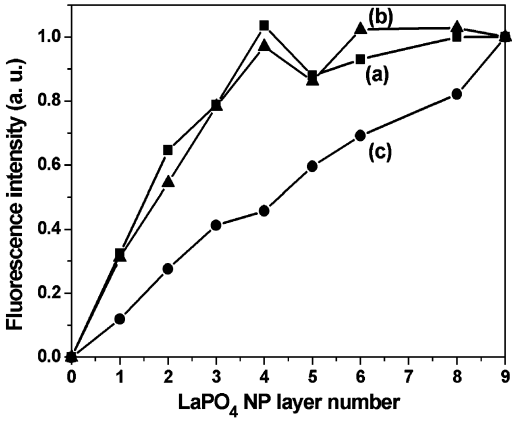

Figure 7. Normalized fluorescence intensity of PSS/NP multilayer films versus the number of NP layers deposited: (a) g-NPs, (b) y-NPs, and (c) r-NPs. An excitation wavelength of 255 nm was used. The fluorescence of the g-NPs, y-NPs, and r-NPs were recorded at wavelengths of 545, 570, and 590 nm, respectively.

Multilayers of PSS and the $LaPO_4$ NPs were formed on QCM and quartz substrates using the LbL technique. The buildup of multilayers was driven by electrostatics, given the opposite charges on the NPs (positive) and PSS (negative). As shown in Figure 6, the layers grew regularly, with an average frequency change, $-\Delta F$, of 650 ± 80 Hz per NP layer for the green and red NPs. This further confirms that the adsorption characteristics of the differently doped NPs are the same. The $-\Delta F$ corresponds to 3500 ± 450 ng cm^{-2},[66] or a NP surface coverage equal to about 1.6 monolayers. This larger than monolayer coverage supports the QCM (Figure 3 inset) and AFM data, also indicating NP infiltration into the topmost polyelectrolyte layers. Regular multilayer film growth for the Ce/Tb-doped (green) and Ce/Dy-doped (yellow) NPs was also observed by UV−vis spectrophotometry (an increase in the cerium absorbance was observed with each NP deposition step) (data not shown). However, as mentioned before, the absorption spectrum of the Eu-doped (red) NPs shows no distinct

absorption bands, thus making it not possible to follow film growth by UV−vis measurements. Both the QCM and UV−vis data demonstrate that the $LaPO_4$ NPs can be incorporated into thin films via the LbL method, allowing the formation of films with controlled NP content.

Consecutive growth of the PSS/NP multilayers was also monitored by following the fluorescence intensity of the films after deposition of each NP layer. The intensity of the films versus NP layer number is plotted for the different NPs in Figure 7. It is evident that the Ce-containing NPs (g-NPs and y-NPs) show behavior (a, b) different from the Eu-doped r-NPs (c): The fluorescence intensity of films comprising g- and y-NPs plateaus after a steep increase for the first four NP layers, whereas for the Eu-doped NPs approximately linear behavior is found for films up to nine NP layers. An influence of increasing absorption of excitation light with increasing film thickness (i.e., layer number) is unlikely because of the small total "extinction" of the films. However, the fluorescence quantum yield of the green and yellow NPs may decrease upon interaction with PSS. It was observed that the addition of PSS to a dispersion of the Ce-containing NPs, or an aqueous solution containing cerium ions, causes a reduction in the original fluorescence intensity of both solutions. This effect was considerably smaller (~80% less) if PSS was replaced by poly(vinyl sulfate), a polyelectrolyte without aromatic groups. The fluorescence intensity of the $LaPO_4$ NP films was also influenced by the humidity of the environment. This effect proved to be largely reversible. Upon drying of the films in an oven at 70 °C, the intensity decreased to 20% of that recorded for the same film after drying with nitrogen. Subsequent immersion of the film in water brought the intensity back up again to 70% of the original value. These data indicate that the fluorescence intensity of $LaPO_4$ NPs is influenced by the polarity at the NP surface as in the experiments conducted, the fluorescence intensity depends on whether the surrounding environment is water or a polymer and whether the polymer contains aromatic moieties. Similar effects (a reduction in fluorescence intensity) also were previously found for the modification of the surface of $LaPO_4$ NPs with tetrabutylammonium hydroxide (ligand).[34] This behavior was explained by a competing process due to the ligand, which results in a decrease in the degree of excitation energy transferred to terbium. It is also known from the literature that the quantum yield of luminescent cerium complexes depends strongly upon the interacting ligands.[69]

The formation of mixed multilayers from differently doped (and hence colored) NPs was also investigated. For these experiments, a combination of the red and green NPs was used. As the r-NPs show weaker fluorescence than the g-NPs, the substrate was first coated with eight layers of r-NPs, followed by a final layer of g-NPs. The final film structure was quartz/PEI/PSS/PDDA/$(PSS/r\text{-}NPs)_8$/PSS/g-NPs. Figure 8 shows the resulting fluorescence spectrum (c) as well as the spectrum for a one-layer film of g-NPs (a) and that for a film containing eight layers of r-NPs (b). For the film containing both NPs (c), the double peak of the r-NPs between 680 and 700 nm and the peak at 545 nm, which is characteristic of the g-NPs, are all clearly discernible in the spectrum. The peaks at 590 and 620 nm are broader as they are a combination of the original peaks at 585 and 622 nm of the g-NPs and the peaks at 590 and 615 nm of the r-NPs. These spectra illustrate that the different NPs retain their individual emission characteristics and that the spectrum for films prepared by the coadsorption of the different NPs is a direct addition of both component spectra.

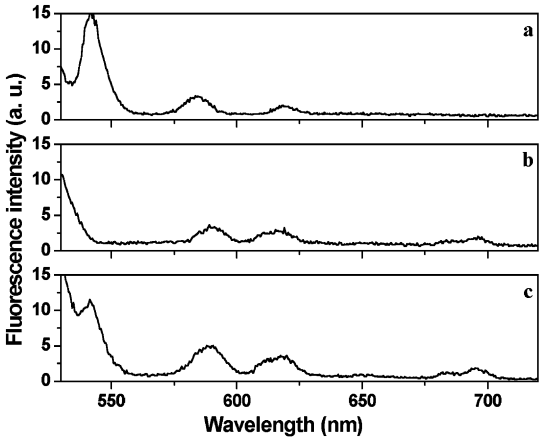

Figure 8. Fluorescence spectra of $LaPO_4$ NP multilayers for a single layer of g-NPs (a), a film with eight r-NP layers [$(PSS/r\text{-}NPs)_8$] (b), and a film containing eight layers of r-NPs and one layer of g-NPs [$(PSS/r\text{-}NPs)_8$/PSS/g-NPs] (c). Spectrum (c) was measured and is a direct addition of the component spectra (a) and (b). All films were prepared on PEI/PSS/PDDA-modified quartz. The excitation wavelength used was 255 nm.

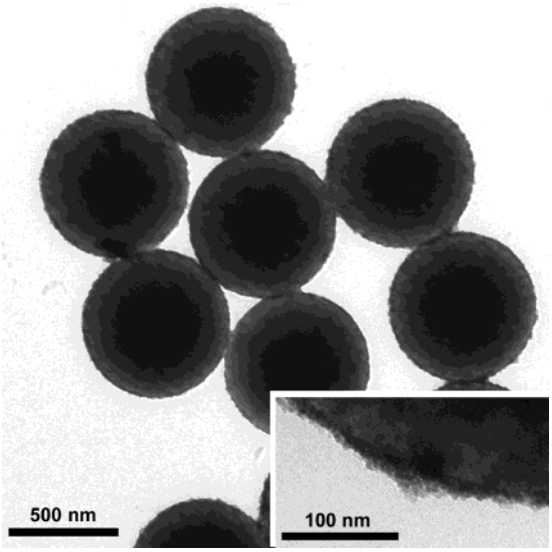

Figure 9. TEM image of PS spheres coated with four layers of polyelectrolyte [$(PDDA/PSS)_2$], one layer of $LaPO_4$ NPs (g-NPs) and one layer of PSS. The higher magnification image in the inset shows the uniform surface coverage of the NPs on the sphere.

$LaPO_4$ NP Coatings (Films) on Colloidal Spheres. A wide field of potential applications (e.g., in the biosciences[70]) is opened by using the $LaPO_4$ NPs to create labeled spheres with tailored optical properties. As the LbL technique is exceptionally versatile concern-

(69) Frey, S. T.; Horrocks, W. D. *Inorg. Chem.* **1991**, *30*, 1073.

(70) Han, M.; Gao, X.; Su, J. Z.; Nie, S. *Nat. Biotechnol.* **2001**, *19*, 631.

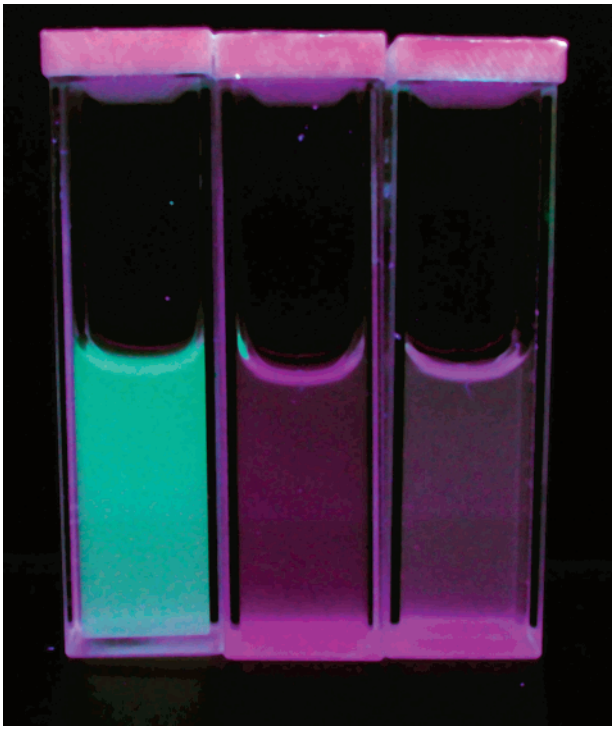

Figure 10. Photograph of dispersions of $LaPO_4$ NP-coated PS spheres. From left to right: coatings comprise one layer of g-NPs, r-NPs, and y-NPs. The PS spheres were premodified with $[(PDDA/PSS)_2]$ and one layer of PSS was adsorbed on top of the NPs. An excitation wavelength of 255 nm was used for illumination.

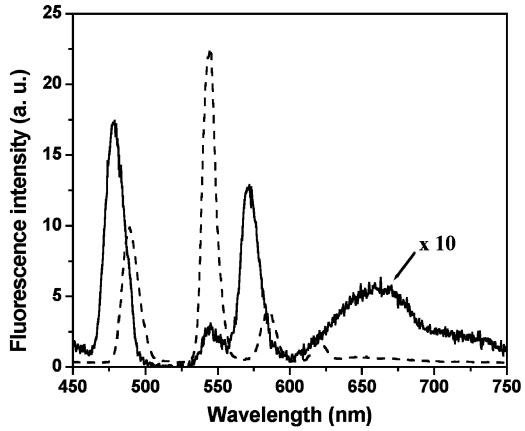

Figure 11. Fluorescence spectra of $LaPO_4$ NP-coated PS spheres. The dashed spectrum corresponds to PS spheres coated with $(PDDA/PSS)_2$/g-NPs/PSS and the solid spectrum to PS spheres coated with $(PDDA/PSS)_2$/y-NPs/PSS. An excitation wavelength of 273 nm was used.

ing the substrates used for deposition, $LaPO_4$ NP/PSS multilayers were grown on PS spheres using the conditions established for the planar supports. The coated PS spheres were imaged by TEM. A dense NP coating, forming a smooth layer around the spheres, was observed, as shown in Figure 9. Dispersions of these NP-labeled spheres show distinct fluorescence, depending on the $LaPO_4$ NPs used, as shown in the photograph (Figure 10). Figure 11 shows the fluorescence spectra of the PS spheres labeled with g- and y-NPs. The characteristic peaks for the different NPs are clearly seen: The suspensions of the NP-tagged spheres show fluorescence peaks at the same positions as the corresponding pure NP dispersions, although the peaks are somewhat broadened due to scattering effects from the PS cores.

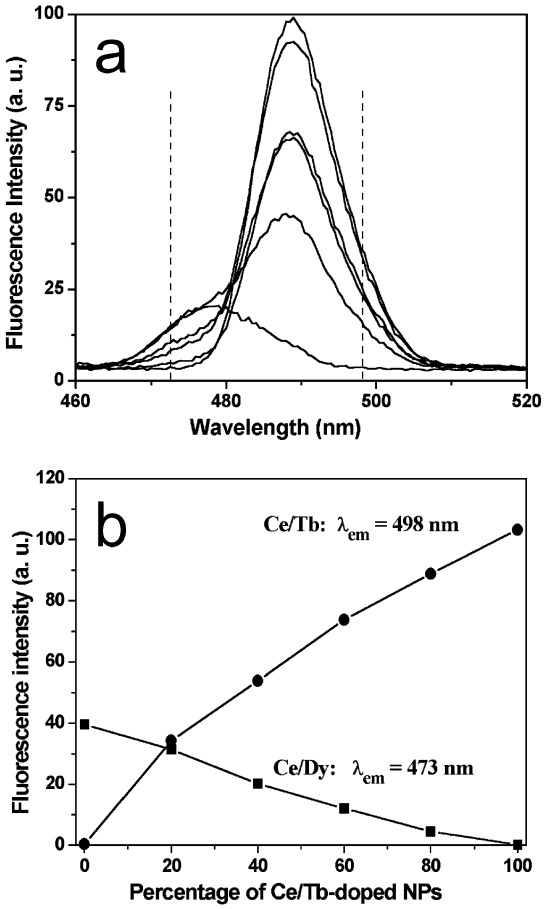

Figure 12. (a) Fluorescence spectra of PS spheres coated with one layer of a mixture of Ce/Tb-doped (green) and Ce/Dy-doped (yellow) NPs; the overall NP concentration was kept constant. The layer composition was $[(PDDA/PSS)_2/NP/PSS]$. An excitation wavelength of 273 nm was used. The growth of the peak at 490 nm (at the expense of that at 479 nm) occurs as the fraction of g-NPs in the adsorption mixture is increased. The dashed lines indicate the wavelengths used for the evaluation in part (b). (b) Plot of the fluorescence intensity of NP-tagged PS spheres versus the composition of the mixture of g-NPs and y-NPs used in the adsorption dispersion. An excitation wavelength of 273 nm was used. To compensate for different concentrations of the PS spheres, the data were corrected by dividing the fluorescence intensity by the optical density of the coated PS dispersion at 900 nm. The squares indicate the fluorescence intensity at 473 nm for y-NPs, while the circles represent the readings at 498 nm for the g-NPs.

A useful property of the $LaPO_4$ NPs to label bigger particles (e.g., beads) is the ability to coadsorb them, while maintaining their individual optical properties once deposited. As shown earlier on planar quartz substrates, the reduction in the interparticle distance upon adsorption has no influence on the spectral peak position of the NPs. As the base material and the surface properties of all three "colors" of NPs are the same, mixtures of the $LaPO_4$ NPs could be readily adsorbed on the microparticles. For each dispersion, the NPs were mixed in a different ratio directly prior to adsorption onto the PS spheres. The preparation of the NP-labeled spheres from the mixtures was conducted as described for the single-component NP adsorption experiments.

For the coated PS spheres, the spectra show that by increasing the concentration of g-NPs in the adsorption solution the peak at 490 nm increases and at the same time the characteristic peak for the yellow NPs at 479 nm decreases (Figure 12a). As a small part of the tails of both peaks overlap, the intensity at the maxima are not suitable for direct evaluation of their individual fluorescence intensities. However, monitoring the intensity at wavelengths of 498 and 473 nm, for the g- and y-NPs respectively, spectral overlap (and hence cross-sensitivity) can be eliminated. In Figure 12b the intensities at these emission wavelengths are plotted versus the NP composition in the adsorption mixture. To minimize the influence of variable concentrations of the PS spheres, the intensities were standardized using the UV-absorption value of the coated PS sphere dispersions at 900 nm. The systematic trend in the data obtained shows the suitability of this approach to label microspheres and tailor their optical properties. Systems based on $LaPO_4$ NP-tagged beads may be interesting alternatives to those of semiconductor nanocrystals embedded in micrometer-sized PS spheres.[70]

Conclusions

We have demonstrated the LbL assembly of single- and multilayer films of defined composition from a new class of fluorescent NPs onto planar supports and beads. The NPs deposited in alternation with oppositely charged polyelectrolytes to form thin films displayed the same fluorescence characteristics as the same NPs in aqueous solutions, with some reduction in the fluorescence observed when alternately deposited with PSS (in the planar films). The fluorescence properties (e.g., intensity) of the nanoparticulate films were found to be tunable by variation of the number of adsorbed $LaPO_4$ NP layers. Additionally, the sequential deposition of differently doped NPs yielded thin films with the characteristic fluorescence of each NP. A valuable feature of the NP-labeled spheres resides in the possibility to detect multiple labels using just one excitation wavelength with no spectral overlap. We are currently using the $LaPO_4$ NPs (with various dopants) and the NP-tagged spheres for bioconjugation and biolabeling studies.

Acknowledgment. Björn Schöler is thanked for the AFM measurements and Christine Pilz for technical assistance. Nanosolutions GmbH is gratefully acknowledged for providing the nanoparticles. S. Haubold, F. Ibarra (Nanosolutions GmbH), and M. Haase (Hamburg University) are thanked for valuable discussions. This work was funded by the BMBF within the framework of the Biofuture program.

CM0212257